

Spectral Domain Method of Moment Analysis of Aperture Coupled Circular Microstrip Patch Antennas

Hamid R. Hassani ^{1*}, M. Jahanbakht ²

Abstract

An aperture coupled circular microstrip patch antenna is analyzed. A full wave spectral domain method of moment along with a reciprocity analysis of a single aperture coupled microstrip element is applied. Both the electric surface current on the circular patch and the equivalent magnetic current on the aperture are considered. Results on effects of different feed line stub length, aperture length, different feed substrate permittivity and thickness on input impedance, resonant frequency and radiation pattern of the antenna and slot are provided.

Keywords: Microstrip Antenna, Aperture Coupled, Circular Patch, Spectral domain

1. Introduction

One of the feeding mechanisms for microstrip patch antennas is through aperture coupling. This feeding structure was originally proposed by Pozar [1] and has received a lot of attention recently. The patch antenna on a dielectric substrate is excited through a narrow non resonant aperture (slot) on the ground plane and the feed circuitry, a microstrip transmission line, is etched on the opposite side of the ground plane conductor, thus, isolating the feed network from the main patch radiator. In this way, no spurious radiation from the feed escapes to corrupt the main pattern of the patch, and leading the way for

¹ Department of Electrical Engineering University of Shahed, Tehran – Iran – hassani@shahed.ac.ir

² Department of Electrical Engineering University of Shahed, Tehran – Iran – jahanbakht@shahed.ac.ir

* Corresponding Author

micro strip antennas to become more suitable for MMIC, wide band and array applications. Furthermore, as the coupling aperture is very small compared to wavelength, radiation field on the feed side is very small.

Although, there has been a number of published papers [2, 3, 4] analyzing the aperture coupled rectangular patch antenna, no full wave analysis of aperture coupled circular patch antennas is in evidence. An approximate analysis based on the cavity model has been reported [5].

In this paper, we present a method of moment analysis of the aperture coupled circular microstrip patch antenna in the spectral domain. This uses the exact Green's functions for the structure and takes into account the surface wave effects on both dielectric substrates. Based on the TM_z modes of a circular cavity [6, 7, 8], appropriate basis functions for the current distribution on the patch are considered.

Input impedance and radiation pattern results for various aperture sizes, location of aperture relative to the microstrip feed line and different substrate permittivities and thicknesses are provided.

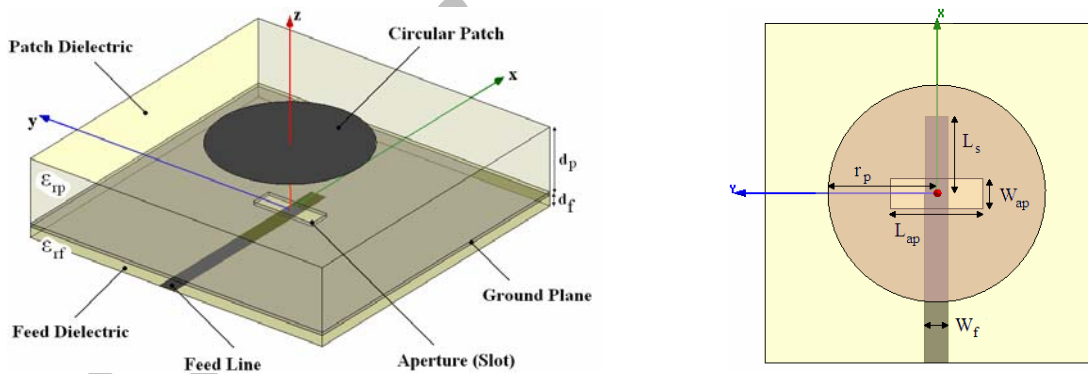


Fig.1 Geometry of aperture coupled circular microstrip patch antenna

II. Theory

The structure of an aperture coupled circular microstrip patch antenna is shown in Fig.1. The spectral domain analysis of the circular patch antenna is basically similar to that of the Rectangular patch antenna formulated by Pozar [2], where details of the formulation can be found. For the purpose of completeness the basic analysis procedure is outlined below.

Similar to the analysis of a slot on a waveguide wall, the effect of a slot discontinuity on the microstrip transmission line can be considered as a series impedance Z . Thus, the equivalent circuit for the aperture coupled patch antenna is as shown in Fig.2. This impedance takes into account the coupling of the patch to the slot and coupling of the feed line to the slot.

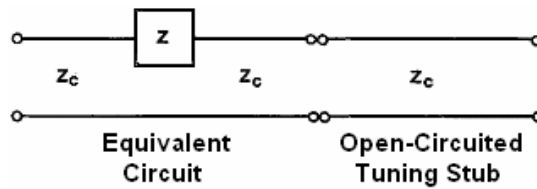


Fig.2 The equivalent circuit of aperture coupled patch antenna as seen by the microstrip line

In this circuit, the series impedance Z is found by applying the reciprocity theorem to the fields of the microstrip line and considering the reflected and transmitted waves on the line and is given by

$$Z = Z_c \cdot \frac{\Delta v^2}{Y^e + Y^a} \quad (1)$$

where Z_c is the characteristic impedance of the microstrip line, Δv is a modal voltage due to the discontinuity of the slot (narrow slot in x direction), Y^e is the self admittance of the slot and Y^a is the admittance due to the patch seen by the slot.

To obtain these parameters the analysis can be divided into two parts, between slot and feed line and between slot and patch.

For the coupling between slot and feed line, from [2], reciprocity theorem can be applied. For a narrow slot, a single piecewise sinusoidal basis function can be used for the electric field (or equivalently a magnetic current) over the aperture, e_x^a . Δv and Y^e are then obtained in space and spectral domain

$$\Delta v = \int_{sa} e_x^a h_y ds = \frac{1}{\sqrt{Z_c}} \int_{-\infty}^{\infty} \tilde{F}_u(k_y) \tilde{G}_{yx}^{HJ}(-k_e, k_y) \tilde{F}_p(k_y) dk_y \quad (2)$$

Where h_y is the magnetic field on the slot due to the current on the feed line, s_a is surface of the aperture and k_e is the effective wave number. Closed expressions can be obtained for the electric and magnetic fields in terms of the relevant Green's functions in Spectral domain. The elements of all the Green's functions required in this analysis are given in the appendix. In (2), \tilde{F}_u and \tilde{F}_p are the spectral domain expressions for the transverse and piecewise sinusoidal current distributions on the feed transmission line and slot and \tilde{G}_{yx}^{HJ} represents the y directed magnetic field due to an x directed electric current on the feed line.

Y^e , the self admittance of the slot can be defined as the reaction between the slot electric field and the magnetic field radiated by slot towards the feed line and patch antenna, expressed as

$$Y^e = \iint_{s_a} e_x^a G_{yy}^{HM} e_x^a ds ds = \int_{-\infty}^{\infty} \tilde{F}_u^2(k_x) \tilde{G}_{yy}^{HM}(k_x, k_y) \tilde{F}_p^2(k_y) dk_x dk_y \quad (3)$$

To obtain Y^a the, admittance due to the patch seen by the slot, the unknown current excited on the circular patch due to the aperture source must be found. This is done using the method of moment

Which starts by writing the boundary condition that?

$$\bar{E}_{\tan}^{scat} + \bar{E}_{\tan}^{inc} = 0 \quad (4)$$

where \bar{E}_{\tan}^{scat} and \bar{E}_{\tan}^{inc} are the tangential components of the scattered electric field due to the currents on the patch and incident electric field on the patch due to the excitation caused by the aperture field, respectively. Using the Green's function technique, this equation can be converted to

$$\int_{sp} (G_{pp}^{EJ} F_{sp} + G_{pq}^{EJ} F_{sq}) ds + \int_{sp} G_{py}^{EM} M_{sy} ds = 0 \quad (p, q = x, y) \quad (5)$$

where \bar{F}_s is the unknown surface current on the patch, G_{pq}^{EJ} is the Green's function representing the p directed E field at the patch interface due to an infinitesimal q directed current element F_q on the patch, M_{sy} is the aperture magnetic current in y direction, G_{py}^{EM} is the Green's function representing the p directed E field at the patch interface due to an infinitesimal y directed magnetic current element at the aperture and s_p denotes the surface of the patch. This integral equation can be solved using the Galerkin's technique in which the unknown current on the patch is expanded in terms of appropriate vector basis functions as

$$\bar{F}_s(x, y) = \sum_{n=1}^N I_n \bar{F}_n(x, y) \quad (6)$$

Where \bar{F}_n are expansion current modes in the x and y direction on the patch and I_n are unknown coefficients to be determined. Substituting (6) into (5) and applying Galerkin's procedure leads to

$$\sum_{n=1}^{\infty} I_n \iint_{sp} (F_{np} G_{qp}^{EJ} F_{mq} + F_{nq} G_{qq}^{EJ} F_{mq}) ds ds_0 + \int_{sp} M_{sy} G_{qy}^{EM} F_{mq} ds_0 = 0 \quad (m = 1, 2, \dots) \quad (7)$$

where \bar{F}_m are the testing functions chosen similar to the basis functions and ds relates to the surface where basis functions apply while ds_0 relates to the surface where testing functions apply. To solve (7), appropriate electric and magnetic current distributions on the patch and slot are required. As before, the non resonant narrow aperture can be replaced with an equivalent magnetic current source, approximated with a single piece-wise sinusoidal mode

$$\bar{M}_s = \hat{y} \left[\frac{\sin k_e (L_{ap} / 2 - |y|)}{W_{ap} \cdot \sin(k_e L_{ap} / 2)} \right] \quad (8)$$

And for the circular patch, the chosen basis functions in terms of the cylindrical coordinates (ρ, φ) , are [7, 8]

$$\bar{F}_i(\rho, \varphi) = \hat{\rho} \beta_{mn} J'_m(\beta_{mn} \rho) \cos m\varphi - \hat{\varphi} \frac{m}{\rho} J_m(\beta_{mn} \rho) \sin m\varphi \quad (9)$$

$$\sum_{n=1}^{\infty} I_n Z_{mn} = V_m \quad (m = 1, 2, \dots) \quad (10)$$

Upon inversion the unknown currents can be obtained

$$\begin{bmatrix} I_{x_1} \\ \vdots \\ I_{x_N} \\ I_{y_1} \\ \vdots \\ I_{y_{N1}} \end{bmatrix} = \begin{bmatrix} Z_{xx_{11}} & \dots & Z_{xx_{1N}} & Z_{xy_{11}} & \dots & Z_{xy_{1N}} \\ \vdots & \vdots & \vdots & \vdots & \vdots & \vdots \\ Z_{xx_{N1}} & \dots & Z_{xx_{NN}} & Z_{xy_{N1}} & \dots & Z_{xy_{NN}} \\ Z_{yx_{11}} & \dots & Z_{yx_{1N}} & Z_{yy_{11}} & \dots & Z_{yy_{1N}} \\ \vdots & \vdots & \vdots & \vdots & \vdots & \vdots \\ Z_{yx_{N1}} & \dots & Z_{yx_{NN}} & Z_{yy_{N1}} & \dots & Z_{yy_{NN}} \end{bmatrix}^{-1} \begin{bmatrix} V_{xy_1} \\ \vdots \\ V_{xy_N} \\ V_{yy_1} \\ \vdots \\ V_{yy_N} \end{bmatrix} \quad (11)$$

Where

[I] is the column vector of unknown patch current coefficients,

[V] is the voltage vector due to the excitation of the magnetic current on the aperture

And

[Z] Is the patch impedance matrix.

$$\begin{aligned} Z_{xx_{mn}} &= \int_{-\infty}^{\infty} \int_{-\infty}^{\infty} \tilde{F}_{n_x}^* \cdot \tilde{G}_{xx}^{EJ}(k_x, k_y) \cdot \tilde{F}_{m_x} dk_x dk_y \\ Z_{xy_{mn}} &= \int_{-\infty}^{\infty} \int_{-\infty}^{\infty} \tilde{F}_{n_y}^* \cdot \tilde{G}_{xy}^{EJ}(k_x, k_y) \cdot \tilde{F}_{m_x} dk_x dk_y \\ Z_{yx_{mn}} &= \int_{-\infty}^{\infty} \int_{-\infty}^{\infty} \tilde{F}_{n_x}^* \cdot \tilde{G}_{yx}^{EJ}(k_x, k_y) \cdot \tilde{F}_{m_y} dk_x dk_y \\ Z_{yy_{mn}} &= \int_{-\infty}^{\infty} \int_{-\infty}^{\infty} \tilde{F}_{n_y}^* \cdot \tilde{G}_{yy}^{EJ}(k_x, k_y) \cdot \tilde{F}_{m_y} dk_x dk_y \end{aligned} \quad (12)$$

$$\begin{aligned} V_{xy_m} &= - \int_{-\infty}^{\infty} \int_{-\infty}^{\infty} \tilde{M}_{sy}^* \cdot \tilde{G}_{xy}^{EM}(k_x, k_y) \cdot \tilde{F}_{m_x} dk_x dk_y \\ V_{yy_m} &= - \int_{-\infty}^{\infty} \int_{-\infty}^{\infty} \tilde{M}_{sy}^* \cdot \tilde{G}_{yy}^{EM}(k_x, k_y) \cdot \tilde{F}_{m_y} dk_x dk_y \end{aligned} \quad (13)$$

From (11), the admittance at the aperture due to the patch can be obtained from

$$Y^a = [V]^t [Z]^{-1} [V] \quad (14)$$

Upon substitution in (1), the series impedance Z of Fig.2 is obtained. Aperture coupled patch antenna is usually tuned with an open-circuited stub of Microstrip line. If the stub length is L_s , using transmission line theory, the input impedance referenced to the aperture would be

$$Z_{in} = Z - jZ_c \cdot \cot(\beta L_s) \quad (15)$$

Where β is the feed dielectric wave number.

More accurate results can be obtained by adding a length extension to L_s to account for fringing fields at the end of the open stub.

Once the current distribution on the patch is known, the field in space can easily be obtained from the relevant Green's functions. To obtain the far field E-plane and H-plane patterns the Stationary Phase Method can be applied to yield

$$\begin{aligned} \bar{E}(\bar{r}) = jk_0 \frac{e^{-jk_0 r}}{2\pi r} \{ \hat{\theta} [\cos \varphi \tilde{E}_x(k_{x0}, k_{y0}) + \sin \varphi \tilde{E}_y(k_{x0}, k_{y0})] \\ + \hat{\phi} [\cos \varphi \tilde{E}_y(k_{x0}, k_{y0}) - \sin \varphi \tilde{E}_x(k_{x0}, k_{y0})] \cos \theta \} \end{aligned} \quad (16)$$

Where \tilde{E}_x and \tilde{E}_y are the spectral domain electric fields in space region given in appendix and k_{x0} , k_{y0} are the stationary phase points.

$$\begin{aligned} k_{x0} &= k_0 \sin \theta \cos \varphi \\ k_{y0} &= k_0 \sin \theta \sin \varphi \end{aligned} \quad (17)$$

III. Results

The above theory was implemented in a software program for calculating the input impedance and radiation pattern of the circular patch.

In computing the integrals, (12) and (13), a significant reduction in the required computer CPU time and more accuracy can be obtained by converting the double infinite $(-\infty, +\infty)$ integrals to polar coordinate system thus resulting in a finite $(0-2\pi)$ and an infinite $(0-\infty)$ integrals (which the finite one can also be reduced to $(0-\pi/2)$ due to the even symmetry of the integrand). For the infinite integral, a quadrature Simpson's rule and for the finite integral, 32 point Gauss quadrature method can be used. On the path of integration for the infinite integral, singularities due to the surface wave excitation must be also taken into account.

Referring to the geometry shown in Fig.1, the fixed parameters of dimensions of such antenna are as follows: $r_p=32.63\text{mm}$, $\epsilon_{rp}=2.55$, $d_p=3.2\text{mm}$, $W_{ap}=1.5\text{mm}$.

In all the cases considered here, calculations were made with 2 basis functions for current on the circular patch for each ρ and ϕ directions and the edge condition was applied to transverse distribution for the aperture and the micro strip feed line.

Increase in the number of basis functions, increases the computational time and was shown to have little effect.

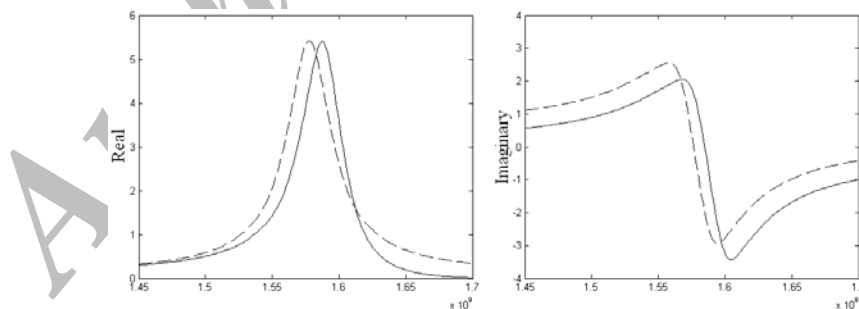


Fig.3 Measured (---), [5], and calculated (—) patch contribution Y^a . $\epsilon_{rf}=2.55$, $d_f=0.8\text{mm}$, $\epsilon_{rp}=2.55$, $d_p=3.2\text{mm}$, $W_f=2.26\text{mm}$, $W_{ap}=1.5\text{mm}$, $L_{ap}=10\text{mm}$, $r_p=32.63\text{mm}$

To check the theory and the software written, a comparison is made between the calculated results of this theory and those measured by [5]. Fig.3 shows this comparison for the patch contribution Y^a of the total input impedance equ. (1). It is clear that the magnitude of the real part and the resonant frequency are very close to measured values.

Fig.4 shows the smith chart plot of the input impedance of the aperture coupled circular patch antenna referenced to the feed line at aperture location for various stub lengths L_s .

The effect of aperture long dimension L_{ap} on the input impedance is shown in Fig.5. It is clear that as the aperture length is reduced, the impedance loci shifts towards the short circuit location, similar to the results of [3], meaning that a decrease of the coupling factor between the feed line and the patch antenna occurs.

Apart from the radius of the circular patch, aperture length also affects the resonant frequency. For design purposes, Fig.6 shows the effect of the aperture length on the resonant frequency and input resistance at resonance.

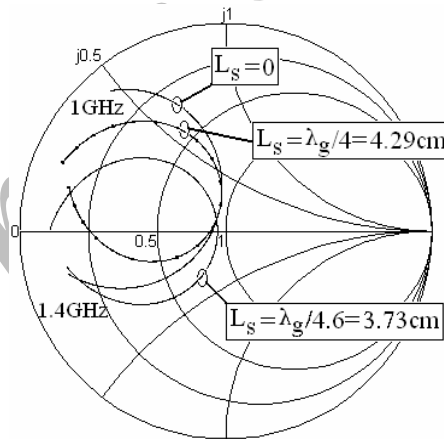


Fig.4 Input impedance for different stub lengths L_s . $\epsilon_{rf}=2.55$, $d_f=0.8\text{mm}$, $\epsilon_{rp}=2.55$, $d_p=3.2\text{mm}$, $W_f=2.26\text{mm}$, $W_{ap}=1.5\text{mm}$, $L_{ap}=20\text{mm}$, $r_p=32.63\text{mm}$

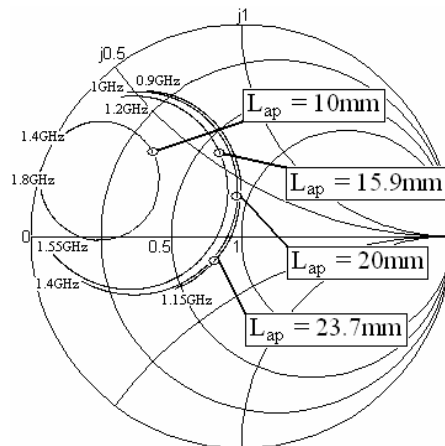


Fig.5 Input impedance as a function of aperture length L_{ap} . $\epsilon_{rf}=2.55$, $d_f=0.8\text{mm}$,
 $\epsilon_{rp}=2.55$, $d_p=3.2\text{mm}$, $W_f=2.26\text{mm}$, $W_{ap}=1.5\text{mm}$, $r_p=32.63\text{mm}$

Earlier it was pointed out that aperture coupled patch antennas are suitable for MMIC application, where active elements can be placed on the feed line directly. This usually requires the feed substrate to have large permittivities, like gallium arsenide. Fig.7 shows the smith chart loci for the input impedance of the antenna with feed substrate having $\epsilon_{rf}=10.2$ for various feed substrate thicknesses.

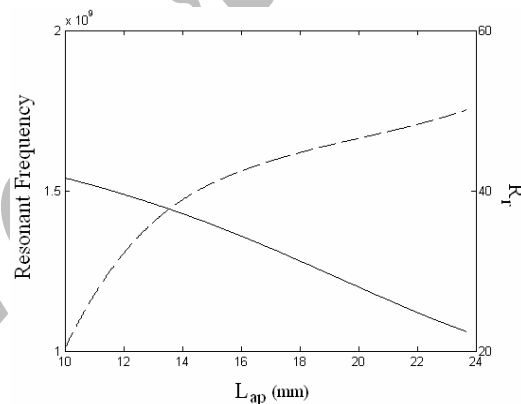


Fig.6 Variation of resonant frequency (—) and input resistance (--) for different aperture lengths L_{ap} . $\epsilon_{rf}=2.55$, $d_f=0.8\text{mm}$, $\epsilon_{rp}=2.55$, $d_p=3.2\text{mm}$, $W_f=2.26\text{mm}$,
 $W_{ap}=1.5\text{mm}$, $r_p=32.63\text{mm}$

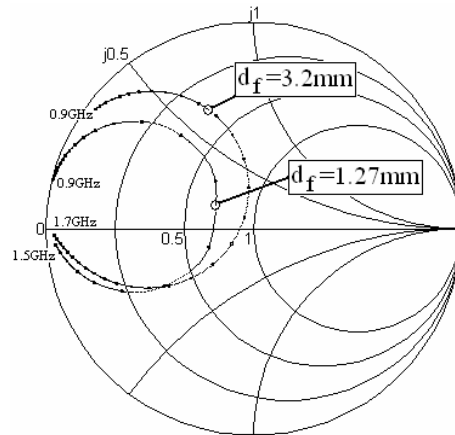


Fig.7 Input impedance for MMIC applications for different feed substrate thicknesses d_f . $\epsilon_{rf}=10.2$, $\epsilon_{rp}=2.55$, $d_p=3.2\text{mm}$, $W_f=1.16\text{mm}$, $W_{ap}=1.5\text{mm}$, $L_{ap}=20\text{mm}$, $r_p=32.63\text{mm}$

Fig. 8 shows the far zone E-plane and H-plane pattern of the aperture coupled circular patch antenna in the upper hemisphere obtained from equ. (16) As summation of the field from the current on the patch and the field from the slot.

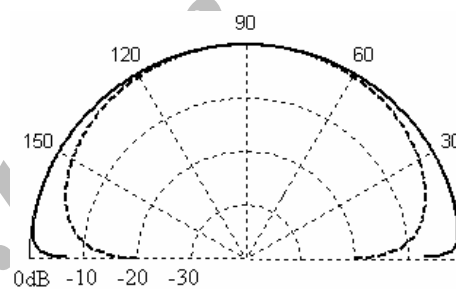


Fig.8 E-plane (—) and H-plane (- - -) far field plots of the aperture coupled circular patch antenna
Of fig.5 with $L_{ap}=20\text{mm}$

IV. Conclusion

Spectral domain analysis of aperture coupled circular patch antenna has been presented. Results were compared with a published experimental data and a very good agreement was found. Input impedance results for various feed line stub length, aperture length and feed substrate permittivity and thicknesses were obtained. Radiation pattern of such a structure was also provided. Results of this study provide a good design guide for such antenna.

Acknowledgment

The author gratefully acknowledges the Iran Telecommunication Research Center (ITRC) for their support and sponsorship.

Appendix

In the analysis, the required Green's functions are

$$\tilde{G}_{xx}^{EJ} = \frac{jz_0}{4\pi^2 k_0} \left[\frac{(k_x^2 k_2 \cos k_1 d + jk_x^2 k_1 \sin k_1 d) \sin k_1 d}{T_e T_m} - \frac{k_0^2 \sin k_1 d}{T_e^{yy}} \right] - \frac{jk_x k_y (\epsilon_r - 1) \sin k_1 d}{4\pi^2 T_e T_m}$$

$$\tilde{G}_{yy}^{EJ} = \frac{jz_0}{4\pi^2 k_0} \left[\frac{(k_y^2 k_2 \cos k_1 d + jk_y^2 k_1 \sin k_1 d) \sin k_1 d}{T_e T_m} - \frac{k_0^2 \sin k_1 d}{T_e} \right]$$

$$\tilde{G}_{xy}^{EM} = \frac{-jk_x^2 (\epsilon_r - 1) \sin k_1 d}{4\pi^2 T_e T_m} + \frac{k_1}{4\pi^2 T_e}$$

And fields in the space are

$$\tilde{E}_x(k_x, k_y) = -k_x k_2 A - \omega \mu_0 k_y C$$

$$\tilde{E}_y(k_x, k_y) = -k_y k_2 A + \omega \mu_0 k_x C$$

Where

$$A = \frac{\epsilon_f^3 k_2}{\epsilon_p j \beta^2 T_{m2}} (k_x \cos(k_1 d) T_1 - k_y \sin(k_1 d) T_2) \tilde{M}_{sy} + \frac{1}{\omega \epsilon_p \beta^2} \left(1 + \frac{\epsilon_f^2 k_1 k_2 \cos(k_1 d)}{T_{m2}} \right) (\tilde{F}_y k_y + \tilde{F}_x k_x)$$

$$C = \frac{k_y k_1}{\omega \beta^2 T_{e2}} (\cos(k_1 d) T_3 - \sin(k_1 d) T_4) \tilde{M}_{sy} + \frac{\mu_0^2 k_1 \sin(k_1 d)}{\beta^2 T_{e2}} (-\tilde{F}_y k_x + \tilde{F}_x k_y)$$

in which $\varepsilon_p = \varepsilon_0 \varepsilon_{rp}$ and $\varepsilon_f = \varepsilon_0 \varepsilon_{rf}$ and

$$T_m = \varepsilon_r k_2 \cos k_1 d + j k_1 \sin k_1 d$$

$$T_e = k_1 \cos k_1 d + j k_2 \sin k_1 d$$

Represent the characteristic equations for surface waves on a grounded dielectric,

$$T_{m2} = -\varepsilon_0 \varepsilon_s k_1 T_m$$

$$T_{e2} = -j \mu_0^2 k_1 T_e$$

$$T_1 = \sin(k_1 d) - j \frac{k_1}{\varepsilon_{rf} k_2} \cos(k_1 d)$$

$$T_2 = \cos(k_1 d) + j \frac{k_1}{\varepsilon_{rf} k_2} \sin(k_1 d)$$

$$T_3 = -j \mu_0 k_1 \cos(k_1 d) + \mu_0 k_2 \sin(k_1 d)$$

$$T_4 = j \mu_0 k_1 \sin(k_1 d) + \mu_0 k_2 \cos(k_1 d)$$

And the Fourier transforms of transverse uniform and piecewise sinusoidal (PWS) functions are

$$\tilde{F}_u(k_y) = \frac{\sin(k_y W / 2)}{k_y W / 2}$$

$$\tilde{F}_p(k_y) = \frac{2k_e [\cos k_y L_{ap} / 2 - \cos k_e L_{ap} / 2]}{\sin(k_e L_{ap} / 2)(k_e^2 - k_y^2)}$$

Where k_e is the effective wave number which is approximately chosen as

$$k_e = k_0 \sqrt{(\varepsilon_r + 1) / 2}$$

A 2-dimensional Fourier transform of the Cartesian basis function (9) on the patch gives

$$\begin{aligned} \tilde{F}_i(k_x, k_y) = 2\pi r_p j^{-m+1} J_m(\beta_{mn} r_p) \{ \hat{x} \left[\cos \alpha \cos m\alpha \frac{\beta_{mn}^2}{\beta_{mn}^2 - \beta^2} J'_m(\beta r_p) + m \sin \alpha \sin m\alpha \frac{J_m(\beta r_p)}{\beta r_p} \right] \right. \\ \left. + \hat{y} \left[\sin \alpha \cos m\alpha \frac{\beta_{mn}^2}{\beta_{mn}^2 - \beta^2} J'_m(\beta r_p) - m \cos \alpha \sin m\alpha \frac{J_m(\beta r_p)}{\beta r_p} \right] \right\} \end{aligned}$$

Where α and β are parameters of coordinate transformation to polar

$$\alpha = \arctan\left(\frac{k_y}{k_x}\right) \quad \text{And} \quad \beta = \sqrt{k_x^2 + k_y^2}$$

References

- [1] D.M. Pozar, "Microstrip Antenna Aperture Coupled to a Microstrip Line", *Electronic Letters*, vol. 21, no. 2, pp.49-50, 1985
- [2] D.M. Pozar, "A Reciprocity Method of Analysis for Printed Slot and Slot-Coupled Microstrip Antennas", *IEEE Trans. Ant. & Prop.*, vol. 34, no. 12, pp.1439-1446, Dec. 1986
- [3] P.L. Sullivan and D.H. Schaubert, "Analysis of an Aperture Coupled Microstrip Antenna", *IEEE Trans. Ant. & Prop.*, vol. 34, pp.977-984, 1986
- [4] X.H. Yang and L. Shafai, "Characteristics of Aperture Coupled Microstrip Antennas with Various Radiation Patches and Coupling Apertures", *IEEE Trans. Ant. & Prop.*, vol. 43, pp.72-78, 1995
- [5] C. Baumer, "Analysis of Slot Coupled Circular Microstrip Patch Antennas", *Electronic Letters*, vol. 28, no. 15, pp.1454-1455, July 1992
- [6] S.A. Long and L.C. S0hen and P.B. Morel, "Theory of the Circular Disk Printed Circuit Antenna", *Proc. IEE*, vol. 125, no. 10, pp.925-928, Oct. 1978
- [7] M. Davidovitz and Y. T. Lo, "Rigorous analysis of a circular patch antenna excited by a microstrip transmission line", *IEEE Trans. Ant. & Prop.*, vol. 37, no. 8, pp. 949-958, Aug. 1989.
- [8] J.T. Aberle and D.M. Pozar, "Analysis of Infinite Arrays of One and Two Probe Fed Circular Patches", *IEEE Trans. Ant. & Prop.*, vol. 38, no. 4, pp.421- 432, Apr. 1990